PROCEEDINGS OF SCIENCE

Centrality dependence of antihyperon production in heavy-ion collisions at high energies

G.H. Arakelyan[†,a] **C. Merino**[b,*] **and Yu.M. Shabelski**

[a] *A.Alikhanyan National Scientific Laboratory (Yerevan Physics Institute), Yerevan, Armenia*

[b] *Departamento de Física de Partículas, Facultade de Física*
Instituto Galego de Física de Altas Enerxías (IGFAE)
Universidade de Santiago de Compostela, Galiza, Spain

E-mail: carlos.merino@usc.es

We analyze in the framework of the Quark-Gluon String Model the experimental data on the production of strange Λ's, and multistrange baryons (Ξ, Ω), and antibaryons, on nuclear targets, as well as on the ratios of multistrange to strange antibaryon production, at the energy region from SPS up to LHC. One remarkable result of this analysis is the manifest violation of the quark combinatorial rules, shown by the experimental dependence on the centrality of the collision of the $\overline{\Xi}^+/\overline{\Lambda}$ and $\overline{\Omega}^+/\overline{\Lambda}$ ratios in heavy-ion collisions.

41st International Conference on High Energy physics - ICHEP2022
6-13 July, 2022
Bologna, Italy

[†] Deceased
[*] Speaker

PoS(ICHEP2022)441

1. Introduction

We compare [1] the results obtained in the Quark-Gluon String Model (QGSM) formalism, with the corresponding experimental data on yields of p, Λ, Ξ, and Ω baryons, and the corresponding antibaryons, in nucleus-nucleus collisions, for a wide energy region, going from SPS up to LHC ranges. We also consider the ratios of multistrange to strange antihyperon production in nucleus-nucleus collisions with different centralities, at CERN-SPS and RHIC energies.

The QGSM [2] is based on the Dual Topological Unitarization, Regge phenomenology, and nonperturbative notions of QCD. In QGSM, high energy interactions are considered as proceeding via the exchange of one or several Pomerons. The cut of at least some of those Pomerons determines the inelastic scattering amplitude of the particle production processes, that occur through the production and subsequent decay of the quark-gluon strings resulting of the cut of the Pomerons.

In the case of interaction with a nuclear target, the Multiple Scattering Theory (Gribov-Glauber Theory) is used. For nucleus-nucleus collisions, the Multiple Scattering Theory allows to consider this interactions as the superposition of independent nucleon-nucleon interactions.

At very high energies, the contribution of enhanced Reggeon diagrams (percolation effects) becomes important, leading to a new effect, the suppression of the inclusive density of secondaries into the central (midrapidity) region. This effect corresponds to a significant fusion of the primarily produced quark-gluon strings.

The QGSM provides a succesful thorough description of multiparticle production processes in hadron-hadron [3], hadron-nucleus [4], and nucleus-nucleus [5] collisions, for a wide energy region.

The production of multistrange hyperons, Ξ^- (dss), and Ω^- (sss), has special interest in high energy particle and nuclear physics. Since the initial-state colliding projectiles contain no strange valence quarks, all particles in the final state with non-zero strangeness quantum number should have been created in the process of the collision. A remarkable feature of strangeness production is that the production of each additional strange quark featuring in the secondary baryons, i.e., the production rate of secondary $B(qqs)$ over secondary $B(qqq)$, then of $B(qss)$ over $B(qqs)$, and, finally, of $B(sss)$ over $B(qss)$, is affected by one universal strangeness suppression factor, λ_s:

$$\lambda_s = \frac{B(qqs)}{B(qqq)} = \frac{B(qss)}{B(qqs)} = \frac{B(sss)}{B(qss)} \,, \tag{1}$$

together with some simple quark combinatorics [6].

Let us define:

$$R(\overline{\Xi}^+/\overline{\Lambda}) = \frac{dn}{dy}(A+B \to \overline{\Xi}^+ + X)/\frac{dn}{dy}(A+B \to \overline{\Lambda} + X) \,, \tag{2}$$

$$R(\overline{\Omega}^+/\overline{\Lambda}) = \frac{dn}{dy}(A+B \to \overline{\Omega}^+ + X)/\frac{dn}{dy}(A+B \to \overline{\Lambda} + X) \,. \tag{3}$$

The produced antihyperons, $\overline{\Xi}^+$ and $\overline{\Omega}^+$, contain valence antiquarks newly produced during the collision. The ratios in eqs. (2) and (3) are reasonably described by QGSM when a relatively small number of incident nucleons participate in the collision (nucleon-nucleus collisions, or peripheral nucleus-nucleus collisions).

The number of quark-gluon strings (cut pomerons) in nucleus-nucleus collisions increases with the centrality of the collision, but if the secondaries are independently produced in a single quark-gluon string, the ratio of yields of different particles should not depend on the centrality.

2. Comparison of QGSM calculations with experimental data

2.1 Fixed Target Energy Data

In Fig. 1 we show the comparison of the QGSM prediction with the experimental data [7] on the dependence of the ratios $\overline{\Omega}^+/\overline{\Lambda}$ (left panel) and $\overline{\Xi}^+$ to $\overline{\Lambda}$ (right panel), on the number of wounded nucleons, N_ω, in Pb+Pb collisions at 158 GeV/c per nucleon. The number of wounded nucleons, N_ω, is directly related to the centrality of collisions. Thus, small values of N_w correspond to peripheral collisions (large impact parameter), while large values of N_w corresponds to central collisions (small impact parameter).

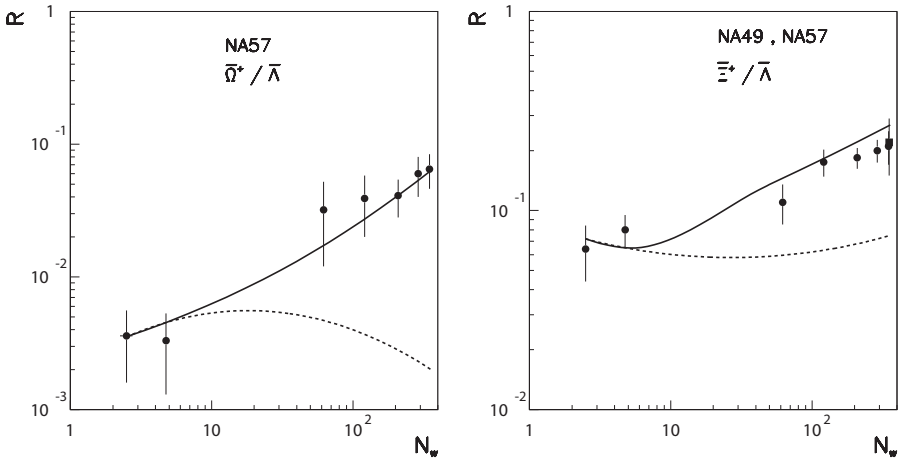

Figure 1: Ratios of $\overline{\Omega}^+/\overline{\Lambda}$ (left panel), and of $\overline{\Xi}^+/\overline{\Lambda}$ (right panel) as functions of the number of wounded nucleons, N_w. The experimental data of Pb+Pb collisions for different numbers of wounded nucleons, N_w (different centralities) measured by the NA57 Collaboration (points), and by the NA49 Collaboration (squares) are presented, and compared with the corresponding QGSM predictions.

At small values of N_w the ratio is practically equal to that in the cases of p+Be and p+Pb collisions, and all they can be correctly described by the QGSM by using a value the of the strangeness suppression parameter, λ_s=0.32. Then, the experimental ratio increases rather fast with the incresing value of N_w, i.e. when we move from peripheral to central Pb+Pb collisions. This behavior is reasonably reproduced by the full line in Fig. 1, that it has been calculated with the value λ_s=0.32 at its left end, and with larger values of λ_s at its right end (see ref. [1] for details). The results of QGSM calculations with a constant value λ_s=0.32, disregarding of the value of the number of wounded nucleons (centrality), N_ω, are shown in Fig. 1 by dashed lines.

Obviously, for small values of N_w, both curves coincide, but when N_w increases the full line also increases in agreement with the data, while the dashed line is practically constant, with exception of small corrections mainly connected to energy conservation. This dashed line shows a very significant disagreement with the experimenatl data at large values of N_w. The difference between the full and the dashed lines for the ratio $\overline{\Omega}^+/\overline{\Lambda}$ in a very central event is of about one order of

magnitude. Such a large difference comes from the fact that the cross section for $\overline{\Omega}$ production is proportional to ${\lambda_s}^3$.

This behaviour in which the value of the strangeness suppression factor λ_s increases with the value of N_w (centrality), indicates that the simple quark combinatorial rules are not valid for central collisions of heavy nuclei.

2.2 RHIC Data

Now we consider the experimental data on midrapidity densities of protons and hyperons in Au+Au collisions measured by the STAR Collaboration [8–12] at RHIC energies, and we compare them with the results of the corresponding QGSM calculations. One can appreciate that, in general, the agreement of the QGSM predictions with the experimental data in this energy region is quite reasonable.

Again, we see here that the value of λ_s for multistrange hyperon production is larger than for the case of Λ and $\overline{\Lambda}$ production. Now this difference is not so large as it is for collisions at lower energies. Moreover, it seems that the difference in the value of the parameter λ_s decreases with the growing of the energy, meaning that the violation of the quark combinatorial rules becomes less important for high energy collisions.

In Fig. 2 we present the comparison of the QGSM predictions with experimental data on the N_ω dependence of the ratios $\overline{\Omega}^+/\overline{\Lambda}$ (left panel), and $\overline{\Xi}^+/\overline{\Lambda}$ (right panel), measured by the STAR Collaboration in the midrapidity region, at $\sqrt{s}$ = 62.4 GeV. Similarly as in Fig. 1, the left end of the full line here was calculated with a value λ_s=0.32, while for the right end larger values of λ_s were used [1]. The dashed line was calculated with a constant value of λ_s=0.32.

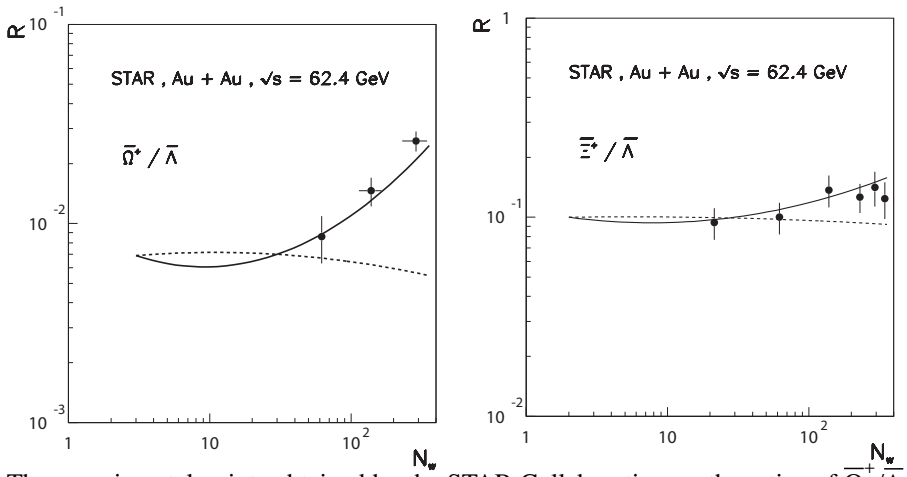

Figure 2: The experimental points obtained by the STAR Collaboration on the ratios of $\overline{\Omega}^+/\overline{\Lambda}$ (left panel), and $\overline{\Xi}^+$ to $\overline{\Lambda}$ (right panel), in Au+Au collisions at $\sqrt{s}$ = 62.4 GeV, at different centralities, as a function of the number of wounded nucleons, N_w, together with the results of the corresponding QGSM calculations (solid curves).

The same calculations for the ratio of $\overline{\Xi}^+/\overline{\Lambda}$ in Cu+Cu collisions at $\sqrt{s}$=200 GeV show again that the violation of the quark combinatorial rules decreses with the growth of the energy of the collision, the difference between the full and dashed lines being of the order of the experimental error bars, at $\sqrt{s}$ = 200 GeV.

Table 1: Experimental data on dn/dy by the ALICE Collaboration of p, $\bar{p}$ central production at $\sqrt{s}$=2.76 TeV [13], of p+$\bar{p}$ central production at $\sqrt{s}$=5.02 TeV [14], Ξ^-, and of Ξ^-, $\overline{\Xi}^+$, Ω^-, and $\overline{\Omega}^+$ production in central Pb+Pb collisions at $\sqrt{s}$=2.76 TeV per nucleon [15], and the comparison with the results of the corresponding QGSM calculations.

Process	$\sqrt{s}$ (TeV)	Centrality	dn/dy (Exp. Data)	dn/dy (QGSM)	λ_s
Pb+Pb $\to p$	2.76	0–5%	34 ± 3	34.604	0,32
Pb+Pb $\to \overline{p}$	2.76	0–5%	33 ± 3	33.898	
Pb+Pb $\to p + \overline{p}$	5.02	0–5%	74.56 ± 0.06 ± 3.75	77.71	0,32
Pb+Pb $\to \Xi^-$	2.76	0–10%	3.34 ± 0.06 ± 0.24	3.357	0,32
Pb+Pb $\to \overline{\Xi}^+$	2.76	0–10%	3.28 ± 0.06 ± 0.23	3.317	
Pb+Pb $\to \Omega^-$	2.76	0–10%	0, 58 ± 0.04 ± 0.09	0.606	0.38
Pb+Pb $\to \overline{\Omega}^+$	2.76	0–10%	0, 60 ± 0.05 ± 0.09	0,601	

2.3 LHC Data

In Table 1 we consider the experimental data on p, $\overline{p}$, and Ξ^-, $\overline{\Xi}^+$, Ω^-, $\overline{\Omega}^+$ production in central Pb+Pb collisions at $\sqrt{s}$=2.76 Tev, and of $p + \overline{p}$ production in central Pb+Pb collisions at $\sqrt{s}$=5.02 Tev, measured by the ALICE Collaboration [13–15], at the CERN LHC.

Here we can see that the strangeness suppression parameter λ_s for Ξ^- and $\overline{\Xi}^+$ production becomes smaller than at RHIC energies, taking the standard value λ_s=0.32. In the case of Ω^- and $\overline{\Omega}^+$ production, the value of λ_s also decreases with respect to the RHIC energy range. Thus we see that the unusually large values of λ_s for central Pb+Pb collisions at 158 GeV/c per nucleon, monotonically decrease with the increase of the initial energy of the collision.

Thus, the experimental data on strange and multistrange particle production show that the value of the strangeness suppression factor to be taken in QGSM to correctly describe those experimental data, it is lower at RHIC and LHC energy ranges, than at SPS (i.e. a smaller enhancement of strangeness production at RHIC and LHC, when compared with that at SPS).

3. Conclusion

We consider the production of hyperons in collisions on nuclear targets in the frame of the QGSM formalism, and we find that the experimental data on the production of hyperons in central collisions of heavy nuclei show a very significant violation, essentially large at CERN-SPS energies $\sqrt{s}$ = 17.3 GeV, of simple quark combinatorial rules, this violation decreasing with the growth of the initial energy of the collision. On the contrary, the corresponding data in proton-nucleus and in peripheral nucleus-nucleus collisions are in agreement with the quark combinatorics theoretical description, by considering one universal and constant strangeness suppression factor.

References

[1] G.H. Arakelyan, C. Merino, and Yu.M. Shabelski, *M*ultistrange hyperon production on nuclear targets, *Phys. Rev.* **D105** (2022) 114013 [hep-ph/2112.01096].

[2] A.B. Kaidalov and K.A. Ter-Martirosian, *P*omeron as quark-gluon strings and multiple hadron production at SPS collider energies, *Phys. Lett.* **B117** (1982) 247.

[3] G.H. Arakelyan, C. Merino, C. Pajares, and Yu.M. Shabelski, *M*idrapidity production of secondaries in pp collisions at RHIC and LHC energies in the quark-gluon string model, *Eur. Phys. J.* **C54** (2008) 577 [hep-ph/0709.3174].

[4] G.H. Arakelyan, C. Merino, and Yu.M. Shabelski, *M*idrapidity hyperon production in pp and pA collisions from low to LHC energies, *Eur. Phys. J.* **A52** (2016) 9 (2016) [hep-ph/1509.05218].

[5] G.H. Arakelyan, C. Merino, and Yu.M. Shabelski, *P*roton and Λ-hyperon production in nucleus-nucleus collisions, *Phys. Atom. Nucl.* **77** (2014) 626, *Yad. Fiz.* **77** (2014) 661 [hep-ph/1305.0388].

[6] G.H. Arakelyan, A.B. Kaidalov, C. Merino, and Yu.M. Shabelski, *P*roduction of strange secondaries in high energy Σ^-A collisions, *Phys. Atom. Nucl.* **74** (2011) 426 [hep-ph/1004.4074].

[7] F. Antinori *et al.*, NA57 Collaboration, *E*nhancement of hyperon production at central rapidity in 158-A-GeV/c Pb-Pb collisions, *J. Phys.* **G32** (2006) 427. [nucl-ex/0601021].

[8] J. Adams *et al.*, STAR Collaboration, *M*ultistrange baryon production in Au-Au collisions at $\sqrt{s_{NN}}$=130 GeV, *Phys. Rev. Lett.* **92** (2004) 182301 [nucl-ex/0307024].

[9] J. Adams *et al.*, STAR Collaboration, *S*caling properties of hyperon production in Au+Au collisiions at $\sqrt{s_{NN}}$=200 GeV, *Phys. Rev. Lett.* **98** (2007) 062301 [nucl-ex/0606014].

[10] B.I. Abelev *et al.*, STAR Collaboration, *Systematic measurements of identified particle spectra in pp, d^+Au and Au+Au collisions fron STAR*, *Phys. Rev.* **C79** (2009) 034909 [nucl-ex/0808.2041].

[11] M.M. Aggarwal *et al.*, STAR Collaboration, *S*trange and Multistrange particle production in Au+Au collisions at $\sqrt{s_{NN}}$=62.4 GeV, *Phys. Rev.* **C83** (2011) 024901 [nucl-ex/1010.0142].

[12] G. Agakishiev *et al.*, STAR Collaboration, *S*trangeness enhancement in Cu+Cu and Au+Au collisions at $\sqrt{s_{NN}}$=200 GeV, *Phys. Rev. Lett.* **108** (2012) 072301 [nucl-es/1107.2955].

[13] B. Abelev *et al.*, ALICE Collaboration, *C*entrality dependence of π, K, p production in Pb-Pb collisions at $\sqrt{s_{NN}}$=2.76 TeV, *Phys. Rev.* **C88** (2013) 044910 [hep-ex/1303.0737].

[14] S. Acharya *et al.*, ALICE Collaboration, *P*roduction of charged pions, kaons, and anti-protons in Pb-Pb and inelastic pp collisions at $\sqrt{s_{NN}}$=5.02 TeV, *Phys. Rev.* **C101** (2020) 044907 [nucl-ex/1910.07678].

[15] B. Abelev *et al.*, ALICE Collaboration, *M*ulyistrange baryon production at midrapidity in Pb-Pb collisions at $\sqrt{s_{NN}}$=2.76 TeV, *Phys. Lett.* **B728** (2014) 216, *Phys. Lett.* **B734** (2014) 409 (erratum) [nucl-ex/1307.5543].